Chemical Engineering Journal 486 (2024) 150103

Contents lists available at ScienceDirect

Chemical Engineering Journal

journal homepage: www.elsevier.com/locate/cej

Semi-interpenetrating network hydrogels-based microcapsule for quorum quenching bacteria biocontainment to enhance biofouling control in membrane bioreactor

Kaixin Yi [a,b], Jinhui Huang [a,*], Haoliang Pang [a], Suzhou Li [a], Zhexi Liu [a], Xia Wang [a], Wei Zhang [a], Chenyu Zhang [a], Si Liu [a], Yanling Gu [c]

[a] College of Environmental Science and Engineering, Hunan University, Changsha, Hunan 410082, China
[b] College of Materials and Environmental Engineering, Changsha University, Changsha 410022, China
[c] College of Materials Science and Engineering, Changsha University of Science and Technology, Changsha 410114, China

ARTICLE INFO

Keywords:
Membrane bioreactors
Quorum quenching
Semi-interpenetrating network
Microcapsule
Biofouling control

ABSTRACT

Microbial quorum quenching (QQ) has been proven to be a sustainable anti-biological fouling strategy for membrane bioreactors (MBR), but the long-term stability and practical application in MBR were uncertain. We reported a novel semi-interpenetrating network (SIPN) hydrogels-based design of QQ bacteria (*Rhodococcus* sp. BH4) encapsulation for both biofouling control and enhancement of organic pollutants removal in MBR. The microcapsule included the alginate core, chitosan thin intermediate compartment and SIPN (sodium alginate / polyacrylamide) shell, which exhibited near-perfect biocontainment, including preventing detectable QQ bacteria escape and improving mechanical strength. The QQ-microcapsules in the MBR demonstrated its significant anti-biofouling effect for treating synthetic wastewater (i.e., membrane fouling was delayed by 233%-280% compared to the control MBR membrane). Meanwhile, the efficiency of phosphorus removal was developed in QQ-microcapsule MBR because of the enhanced phosphorus removal triggered by the flocculation of polyacrylamide (PAM) fraction in SIPN. This promising QQ media brings the broad potential for biofouling control and long-term efficient operation in actual MBR wastewater treatment.

1. Introduction

The commercial use of membrane bioreactors (MBRs) has increased dramatically over the last two decades due to the advantages of high quality and compactness in wastewater treatment (Shi et al.,2019a). However, biofouling, i.e., the loss of filterability caused by the formation of a natural biocake on the membrane surface, has still not been effectively addressed, even significantly weakening its efficiency [1,2]. It was widely reported that biofouling is closely associated with microbial cell-to-cell communication which is called quorum sensing (QS) [3]. And quorum quenching (QQ) has been regarded as a fundamental approach that inhibits QS mainly through the degradation of signaling molecules, which gradually developed mainly from the use of enzymes [4], bacteria [5,6] and fungi [7]. Various types of QQ media were designed successfully and applied to mitigate MBR membrane biofouling [8–10].

As a widely used strategy, chemical biocontainment uses chemical barriers to safeguard the survival of microorganisms and to impede their escape [11]. Hydrogels are desirable materials for providing target microorganisms nutrients, which enabled living immobilization, cell growth [12], sensing [13], and also protecting against environmental stress [14]. Sodium alginate (SA) is a natural polysaccharide that can form hydrogels in divalent cationic solutions such as Ba^{2+} and Ca^{2+}, which has been used in various biomedical applications [15,16] due to the favorable biocompatibility, mild gel conditions and low cost. However, the alginate matrix is still restricted by disintegration and weak mechanical strength. Naturally, the properties of hydrogel were optimized by physical and chemical modification. Kim et al. successfully implemented QQ-bacteria immobilized alginate cores coated with polymeric film layers, but the unevenness of the membrane thickness may lead to core deviation or detachment in the MBR aeration environment [17].

However, aiming at the problems of insufficient mechanical properties and difficult standardization of production, we devoted to investigating a kind of QQ immobilized carrier with strong mechanical

* Corresponding author.
E-mail address: huangjinhui@hnu.edu.cn (J. Huang).

https://doi.org/10.1016/j.cej.2024.150103
Received 4 December 2023; Received in revised form 26 February 2024; Accepted 28 February 2024
Available online 11 March 2024

property, superior performance and controllable preparation process. Polymeric semi-interpenetrating network (SIPN) membrane layer are typically composed of two polymers, and one of which is cross-linked in the close presence of the other. The synthesis of SIPN is an effective approach for the manufacture of superior multifunctional "alloys" cross-linked polymer, and it has been reported that SIPN-type hydrogels of polysaccharides have been widely used in encapsulation intensifying [18,19]. Sodium alginate/polyacrylamide (SA/PAM) SIPN polymer-based protective shell combines both a stretchy polymer network (polyacrylamide) and an energy dissipation network (alginate, through the unzipping of ionic crosslinking between polymer chains), yet remains permeable for small molecules [20]. In addition, a mold is applied to make the shell coating uniform and spherical-shaped [21]. Furthermore, in order to keep the QQ core free of irreversible damage (most are the death of bacteria caused by exposure to toxic substances) during the manufacturing operation, a thin layer of chitosan with excellent biodegradability was chosen as the intermediate septum layer since the amino of chitosan molecule can trigger polyelectrolyte reaction with carboxyl in alginate molecular to form a semipermeable membrane on the surface of alginate cores [8]. And it is the first attempt to apply this SIPN structure to bacterial immobilized in a wastewater treatment system, the mold coating method is creatively applied to standardize the product. Moreover, polyacrylamide (PAM) is one of the most widely used coagulant in wastewater treatment, and could even chemically enhance the primary treatment [22]. Therefore, SA/PAM based capsule has great potential for application in sewage treatment systems.

In this study, a simple, inexpensive, standardized immobilized product of QQ microcapsule was developed by crosslinking/embedding/ mold casting method. And the design for QQ encapsulation consists of three parts: (1) a QQ-bacteria hydrogel core, (2) a chitosan layer to insulate against possible toxicity and (3) a tough SIPN (sodium alginate / polyacrylamide) hydrogel shell to protect the BH4 core. Herein, physical (swelling ratio and weight change) and chemical stability tests showed that our core–shell QQ microcapsule achieved near-perfect biocontainment and protect the encapsulated bacteria from damage caused by the outside environment, yet retains permeability to small molecules. Finally, we showed that the QQ microcapsule could exert QQ effect to control membrane biofouling and partially enhance phosphorus removal in MBR continuously, which provided another perspective for the practical application.

2. Materials and methods

2.1. Manufacturing the microcapsules

Rhodococcus sp. BH4 was incubated in Luria-Bertani (LB) culture at 30 °C. After 24 h, the culture medium was centrifuged and washed with sterile water, then re-suspended with sterile water. Sterilize 3 % (w/v) sodium alginate at 115 °C for 15 min, then mix with the bacteria liquid (0.1g bacterial per 10g sodium alginate solution). The core was then formed by syringes bacteria–alginate premix, then soak in 5 % calcium chloride solution to form spheres. Next, the core was immersed in 0.4 % (v/v) chitosan solution (0.4 % glacial acetic acid, pH = 6) for 30 mins, the SA-C bead was obtained after washing three times with 0.9 % NaCl solution and deionized water, respectively. The fast-curable prehydrogel solution composed of 25 % acrylamide, 5 % N-methylene biscrylamide, 2 % alginate, 0.046 % ammonium persulfate and 0.05 % N,N,N',N'-Tetramethylethylenediamine (TEMED) was injected into the mold plate with 5 mm diameters, then the previous cores were dipped into the center of mold and coated with the SA/PAM polymer blend layer. To stabilize the shell, the microcapsule was immersed in the 2-Morpholinoethanesulphonic acid (0.1 M MES, 0.5 M NaCl, pH 6.0), crosslinked fluid including 0.00125 % 1 - ethyl-3-(3-dimethyl amino propyl) carbon imide (EDC), 0.000375 % N - butyl hydroxy dimide and 0.00075 % adipic hydrazine (ADH) for 3 h, and then the SA-C-SIPN microcapsule was prepared successfully, and the microcapsule without chitosan was called SA-SIPN.

2.2. Physical stability measurements of the manufactured microcapsules

To evaluate the physical stability of the core–shell microcapsules, swelling characteristics and weight change of hydrogels were tested. 30 vacant microcapsules were soaked in deionized water for 25 days and gently shaken [23]. During the monitoring period, the expanded hydrogel was gently removed from the solution at regular intervals. The diameter of the microcapsules were determined by vernier calipers after removing the surface moisture. The volume of the hydrogel capsule is defined by following Eq (1). The swelling ratio (SR) is calculated as follows:

$$V = \left(\frac{4}{3}\right)\pi\left(\frac{D}{2}\right)^3 \quad (1)$$

$$SR = \left(\frac{V_t}{V_0} - 1\right) \times 100\% \quad (2)$$

V is the volume of microcapsules, cm^3; v_t is the volume of microcapsules at time t, cm^3; V_0 is the volume of microcapsules at time 0, cm^3; d is the diameter of microcapsules, cm

In the weight change test, 30 microcapsules of each kind of microcapsules were placed in a blast oven and dried for 30 min at 37℃, and the initial mass of the capsules after drying was recorded immediately as W_0. Then, these microcapsules were placed in deionized water and continued in the simulated aeration environment within the MBR. The gel beads were removed at 0d, 1d, 3d, 5d, 10d, 15d, 20d and 25d, respectively. The moisture on the surface was wiped and placed in the oven for 30 min at 37℃, weigh and record as W_t, the weight change was evaluated as follows eq (3).

$$\text{Weight change} = \frac{W_t}{W_0} \times 100\% \quad (3)$$

2.3. Chemical stability measurements of the manufactured microcapsules

A chemical stability test was derived to evaluate the tolerance to the harsh chemical environment. A buffered EDTA solution (30 mM EDTA, 55 mM sodium citrate and 0.15 M sodium chloride) was configured for harsh chemical environments. Since EDTA is known to be a strong complexing agent with calcium ions [24] can easily disintegrate alginate core containing calcium ions. The EDTA solution with four types of beads added was lightly stirred and incubated. To test the chemical stability, 3 mL were removed from the suspension every 10 min and the absorbance at 600 nm was measured to determine the leak of collapsed bead cells.

2.4. Study of quorum quenching efficiency of the hydrogel

The activity of QQ was evaluated according to the degradation rate of C8-HSL (N-octanoyl-L-Homoserine lactone, a typical AHL signaling molecule), and the concentration of C8-HSL was quantified by Liquid Chromatograph Mass Spectrometer (LC-MS) coupling with a time of flight mass spectrometry (Agilent, California, USA) [25]. 1 % (v/v) QQ microcapsules were placed in 10 mL of C8-HSL solution (200 ng/mL, Tris-buffer solution as solvent) and agitated in a shaker at 200 rpm. Then 100 μL of each solution was sampled at 0, 30, 60, 120, 240 and 480 min and detected. In addition, the QQ activity of vacant microcapsules was also determined. QQ activity was characterized by the degraded C8 concentration as a percentage of the original concentration. In long-term quorum quenching activity test, the activated sludge was inoculated in two sequencing batch reactors (200 mL) with 1.5 L/ min continuous aeration. The artificial wastewater (COD was 500 mg/ L) was replaced every day to improve the stability of the system. 1 % (v/v) QQ microcapsules (SA-SIPN and SA-C-SIPN) were added into the two reactors,

respectively. We then periodically detected quorum quenching activity (Defined as the quorum quenching activity in 8 h) of microcapsules over a period of four months [26].

2.5. Membrane biofilm formation experiments

Considering the QQ microcapsules for mitigation membrane biofouling formation involves two aspects (physical scrubbing effect and QQ activity) [27]. Vacant microcapsules and QQ microcapsules were placed into batch reactors to characterize the combined effect, respectively. 9 sequent batch reactors were set and inoculated with 100 mL activated sludge and kept 500 mg/L COD. The PC plate was placed vertically in the reactors and three parallel PVDF flat membrane (Φ25) fixed on the PC plate, 20 microcapsules of each type (four kinds of vacant microcapsules) were placed in reactors and keep continuously aerated (1.5 L/min). After 5 days, the PVDF samples were removed and stained (10 mL of 0.1 % crystal violet) for 30 min. The specimens were immersed in 10 mL of ethanol solution for 30 min and then discarded. Finally, the concentration of ethanol was measured at OD 590 with a UV–Vis spectrophotometer. The mass of the biofilm formed was defined as the absorption value [28].

2.6. Membrane bioreactors operation

Three submerged MBRs with a working volume of 4.5 L were continuously operated in parallel. That is, the control reactor without microcapsule, the vacant- microcapsule reactor and the QQ-microcapsules reactor. Hollow fiber membranes (KOCH, USA) were made of polyvinylidene fluoride (PVDF). The proportion of vacant-microcapsules or QQ-microcapsules inserted into each MBR was 2 % (v/v). The flux of each reactor was 12 L/m^2/h controlled by a peristaltic pump, and with an aeration rate of 2.0 L/min [29]. The synthetic wastewater consists of the following components (mg/L): glucose, 400; peptone, 115; yeast extract, 14.0; KH_2PO_4, 21.8; $(NH_4)_2SO_4$, 105; $FeCl_3{\cdot}6H_2O$, 0.13; $MgSO_4{\cdot}7H_2O$, 32.0; $MnSO_4{\cdot}5H_2O$, 2.88; $CaCl_2{\cdot}2H_2O$, 3.25; $NaHCO_3$, 256. The concentration of the media applied to each reactor was 0.5 % (v/v). The transmembrane pressure (TMP) was continuously monitored to evaluate the degree of biofilm in each MBR during operation. The period was considered to end when the TMP reaches 40 kPa (Yi et al., 2022). At the end of the first cycle, the used filter membranes were cleaned with 1000 ppm NaOCl solution and then re-immersed in the reactor separately for the next cycle. In the second cycle, no microcapsules were added to control MBR, 1 % (v/v) vacant-microcapsules (SA-C-SIPN) and QQ-microcapsules (SA-C-SIPN) were added to other two reactors, called vacant-microcapsules MBR and QQ-microcapsule MBR, respectively. The experimental setups continuously operated until the TMP of the QQ-microcapsule MBR reached 40 kPa. Then, the procedure of the second stage was repeated after mixing and redistribute of activated sludge.

2.7. Confocal laser scanning microscopy (CLSM)

After the second cycle, the membrane modules were removed and the 5 cm membrane filaments were intercepted. And biofilm on the membrane surface was stained with MKBio SYTO 9/PI live/dead bacteria double stain kit (Maokang Biotechnology, Shanghai) for 15 min in the dark according to the operation manual. The distribution of living/dead cells of membrane biofilm was observed with confocal laser scanning microscopy (CLSM) (Olympus FV1200). The excitation light of live and dead bacteria is set at 488 nm, and the light received by live bacteria is 530 nm, and the light received by dead bacteria is 635 nm, respectively.

2.8. Analytical methods

Mechanical strength was monitored by an electronic universal testing machine (MTS, USA). 30 microcapsules were placed on testing machine and the average value was analyzed (probe: P/0.5). The starting force maintained for 5 g and test speed was 0.5 mm/s.

The thermal analysis was performed by a thermosgravimetric analyzer (Hitachi, Japan). 5 mg microcapsule sample was dried and then heated from room temperature to 800 °C at a rate of 20 °C/min under nitrogen environment.

Fourier transform infrared spectroscopy (FTIR) was performed to confirm the formation of the intermediate membrane layer and the semi-interactive protective layer characterization. Vacant SA, SA-C and chitosan powder, acrylamide monomer and polyacrylamide outer layer were dried in an oven at 60 °C, then ground into powder and then analyzed by FTIR with the wavelength from 4000 cm^{-1} to 400 cm^{-1} [30].

Mass transfer efficiency experiments were carried out in methylene blue solution [31]: 20 microcapsules of SA, SA-C, SA-SIPN, and SA-C-SIPN were placed into the methylene blue solution (2.5 %, 200 mL), and shake at 150 rpm. Samples were taken at 0, 5 min, 15 min, 30 min, 60 min and 120 min and their absorbance at wavelength of 665 was measured, then calculate the mass transfer efficiency of different microcapsules (Eq. (4)).

$$ME(\%) = \frac{A_0 - A_t}{A_0} \times 100\% \tag{4}$$

ME is mass transfer efficiency, %; A_0 is the initial absorbance of methylene blue solution; A_t is the absorbance of the solution at time t.

Chemical oxygen demand (COD), TN (NH_4^+) and PO_4^{3-} were measured according to standard methods [32].

The concentration of SMP and EPS in the sludge mix of each MBR was extracted and tested at the end of second cycle according to the previous study (Huang et al, 2019b).

To observe each membrane layer of the capsule, we cut SA-C-SIPN (SA/PAM) in half and separated the SIPN membrane from the core. These parts were pre-frozen in a −20 °C freezer for 48 h and then freeze-dried for 6 h. Imaging was performed by scanning electron microscope (SEM, ZEISS Sigma 300) [33].

3. Results and discussion

3.1. Characterization of the core–shell hydrogel microcapsules

A mixture of liquid cultured BH4 and alginate was dropped into the crosslinker to form spheres. Then, the alginate core was coated with a tough Semi interpenetrating network (SIPN) hydrogel (polyacrylamide-alginate hydrogel layer) in a mold. Specifically, in order to block the toxicity of organic solvents TEMED to internal bacteria during shell preparation [8], we designed a three-layer structure with a thin layer of chitosan which possessed stronger physical containment and biocompatibility, Fig. 1 illustrated the preparation process. As shown in Fig. S1 and Table S1, four kinds of microcapsules were translucent and global in shape with diameters ranging from 3.45 to 5.94 mm. The densities were approximately 1.0 g/ mL, hence the capsules could float in the activated sludge mixed liquor by circulating aeration to facilitate the scouring of the membrane module.

SEM images were used to characterize the morphology of the core–shell hydrogel-bacteria beads. All samples were dehydrated after vacuum drying. As can be seen from Fig. 2a-2c, alginate and polyacrylamide showed excellent compatibility in SIPN and a thin homogeneous layer was successfully formed. The surface of the middle layer (2c, i.e. Chitosan) and outer shell (SA/PAM) presented a dense microporous structure which is desirable for the biocontainment and mass transfer process of nutrients. Moreover, as can be seen in Fig. 2a-2d, a stable core–shell structure was formed, although the inner shell is slightly deformed due to the lyophilization.

Next, we tested the FTIR spectra of sodium alginate, chitosan, acrylamide (AM) and SIPN (SA-PAM) hydrogel, respectively. As

Fig. 1. The process of core–shell encapsulation of *Rhodococcus* sp. BH4. Droplets of 2.5% alginate with *Rhodococcus* sp. BH4 was crosslinked in a calcium solution to form the soft core of the beads, which were then coated with an interlayer of chitosan, and then coated with alginate/polyacrylamide to form a tough hydrogel shell in the mold.

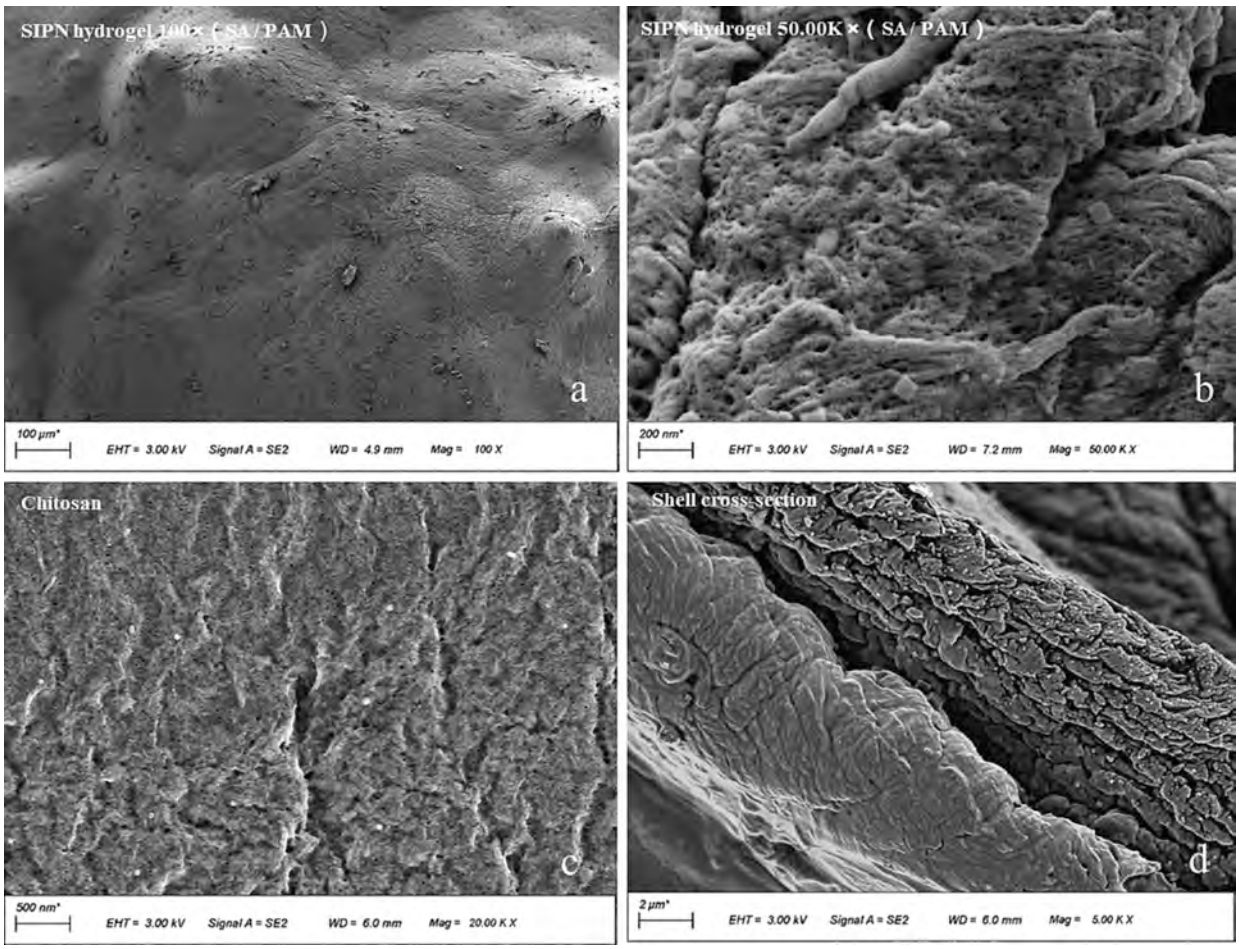

Fig. 2. (a) SEM images of SIPN (sodium alginate- polyacrylamide) shell, ×100. (b) SEM images of SIPN shell, ×50 K. (c) cross-section of SA-C-SIPN microcapsule, ×5K.

described in Fig. 3, the peak at 3407 cm^{-1} is associated with the stretching vibration of the OH group, and the peak at 2927 cm^{-1} reflects the CH stretching of the aliphatic group, which were the characteristic peaks of sodium alginate. The energy band at 1615 cm^{-1} is the asymmetric vibration of v (–coo group), while the energy band at 1418 is attributed to the v (coo) symmetric vibration. In the spectra of chitosan, 2875 cm^{-1} is the CH_2 asymmetric stretching vibration; 1656 cm^{-1} is C = O in the amide group; amide I vibration peak at 1656 cm^{-1} and amide II vibration peak at 1598 cm^{-1} [34,35]; The amino group characteristic absorption peak at 1156 cm^{-1}. the symmetric vibration peak of N-H at 3406 cm^{-1} in sodium alginate-polyacrylamide, 2930 cm^{-1} and 1403 cm^{-1}, the stretching vibration absorption peak of $–CH_2$ at 1657 cm^{-1}. The bands at 3352–3360 cm^{-1} (νas NH_2) and 1666–1679 cm^{-1} (n C = O) are characteristics of the acrylamide unit. All these peaks shift to some extent in SIPN, indicating the electrostatic interaction between polyacrylamide and sodium alginate functional groups in SIPN. Accordingly,

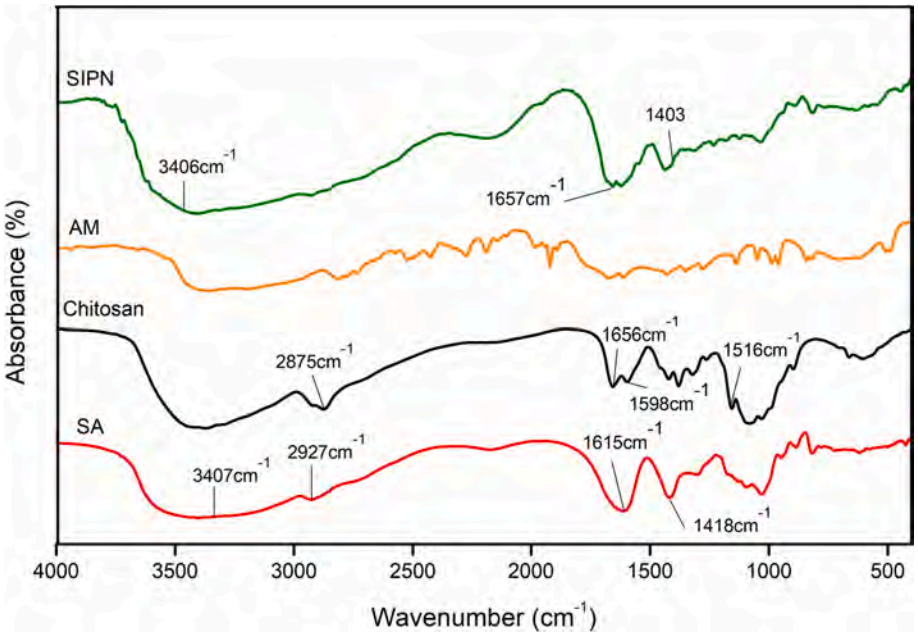

Fig. 3. FTIR of sodium alginate, chitosan, acrylamide and polyacrylamide.

the peak of OH stretching vibration in sodium alginate spectra and the peak of doublet N–H stretching vibration in polyacrylamide spectra overlapped at 3406 cm^{-1} in SIPN [36]. Similarly, the peak of COO– of sodium alginate (1615 cm^{-1}) and primary amide C = O absorption band of polyacrylamide (1675 cm^{-1}) overlapped at the 1657 cm^{-1} peak of SIPN. N–H stretching vibration of polyacrylamide at 1351 cm^{-1} was also shifted to 1335 cm^{-1} in SIPN.

3.2. Thermal analysis

Thermal analysis was conducted to evaluate the thermal stability. Fig. 4 showed the thermogravimetric analysis (TGA) and differential thermal analysis (DTA) of four types of microcapsules. Significant mass loss (about 70 %) was observed for the four types of microcapsules from 30℃ to 120℃, indicating the loss of weakly bound water molecules from the gel network. During 120℃- 650℃, the mass loss of the microcapsules reached 96 % (SA), 95 % (SA-C), 87 % (SA-SIPN) and 93 % (SA-C-SIPN), then gradually stabilized, respectively. In the case of sodium alginate cores, it is mainly the breakage of mannuronic and glucuronic acid fragments at 230-275℃ [37], while the breakage of the main polymer chains happened at 280-600℃. Moreover, the main polymer chain of polyacrylamide was degraded at 230-260℃ and the degradation of the entire structure occurs from approximately 360 ℃ [38]. It was presented in the DTA curve that exothermic peaks appeared around 190 ℃ in SA and SA-C, which was shifted to 199℃ and 221℃ after loading the SIPN. The results demonstrated that membrane layer cladding with SA/PAM increased thermal stability.

3.3. Living/dead bacteria distribution and mass transfer analysis in microcapsules with different membrane layers

The living/dead bacteria distribution in the microcapsule was

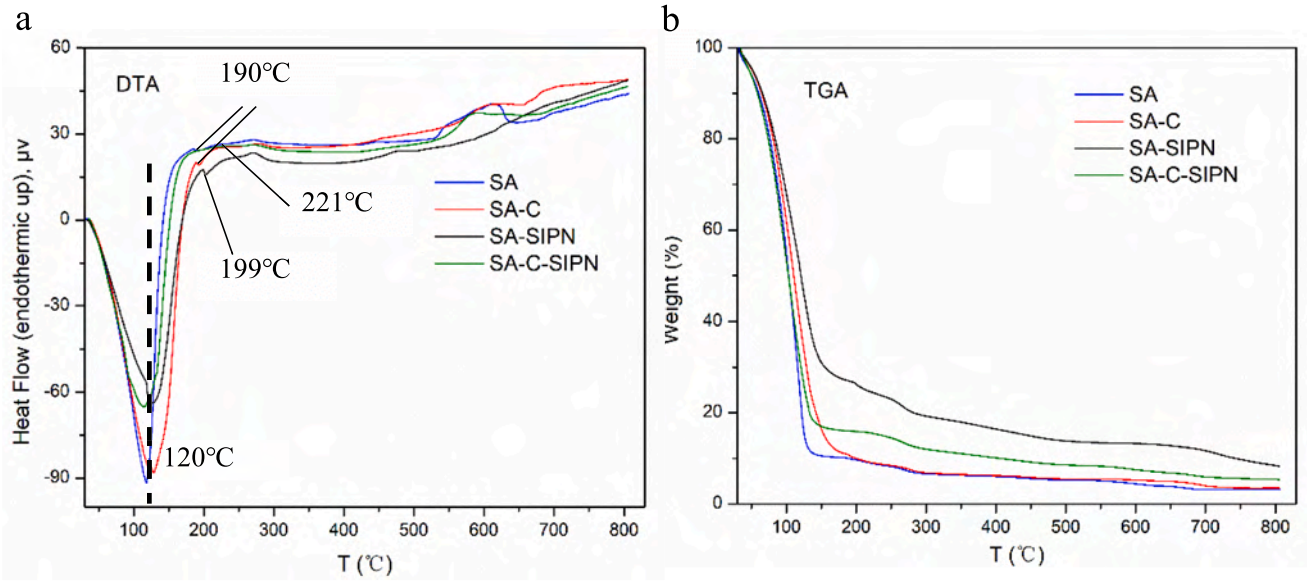

Fig. 4. DTA and TGA of the SA, SA-C, SA-SIPN and SA-C-SIPN microcapsules.

analyzed after the staining with live/dead bacteria double strain kit. The CLSM images of SA-SIPN and SA-C-SIPN microcapsules were shown in Fig. 5. In the SA-SIPN microcapsules without middle layer, a certain number of dead cells (red) were observed at peripheral of SA core, which was due to the organic solvent may directly contact the quorum quenching bacteria, and even cause the death of cells during polymerization and encapsulation process of propionamide monomer. However, in the CLSM image of SA-C-SIPN microcapsules with a mid-spacer layer, the red part was very few, indicating that the design of the chitosan interlayer plays a role in protecting bacteria from the damage caused by SIPN casting solution. The protection of internal QQ bacteria in SA-C-SIPN microcapsules attempts to enhance quorum quenching stability.

Bacteria immobilization carrier should be relatively unobstructed mass transfer channel, which ensure the transport of nutrients and metabolic product of bacteria. In previous study, adsorption method is often applied to simulate mass transfer processes for visualization purposes [39]. As shown in Fig. S2, the basic mass transfer efficiency of SA, SA-C, SA-SIPN and SA-C-SIPN microcapsules were 45 %, 52.7 %, 47.1 % and 46.7 %, respectively. The highest mass transfer efficiency with SA-C was mainly because the thin layer of chitosan does not cause obvious mass transfer obstruction and even provides more adsorption sites for methylene blue. The three-dimensional structure of sodium alginate is very conducive to the transfer and diffusion of materials, and high porosity of the chitosan film layer further improved the mass transfer efficiency. After coating the relatively dense SIPN shell, mass transfer efficiency has no obvious change. Therefore, the microcapsules with multi-layer core–shell structure could effectively ensure the basic internal mass transfer.

3.4. Physical stability of core–shell QQ microcapsule

As shown in Fig. 6, the swelling rates (SR) of SA and SA-C beads increased rapidly to as high as 120 % and 130 % and then achieved swelling equilibrium on the 15th day. For the SA-SIPN and SA-C-SIPN microcapsules, the time for the equilibrium was getting shorter (5 days) with a reduced swelling ratio (about 20 %). The higher swelling rates of SA and SA-C may be due to the high hydrophilicity of alginate and chitosan. The increased electrostatic repulsion in the network, as the carboxyl functional group of alginate ($COO\text{-}Na^{+}$) is negatively charged, resulted in the improvement of water absorption properties of SA and SA-C. According to previous studies, higher cross-linking degree triggered the formation of a tighter network. And during the swelling process, the dense SIPN layer was rapid shrinkage due to hydrophobic interaction between various hydrophobic groups on its surface, thereby showing swelling rate [40]. Therefore, the SIPN structure membrane was well cross-linked in the production process, forming a stable protective layer.

The physical stability was characterized by the weight change of the beads under aeration conditions. This setup was designed to simulate the aeration environment in wastewater treatment. The weight change of SA and SA-C beads increased in the 3 days due to water absorption and swelling, and then gradually collapsed within the next 17 days. However, the weight change of SA-SIPN and SA-C-SIPN beads was no more than 27 % through the analysis of the experimental data. The microcapsules absorbed water and stored it in the pores of the hydrogel SA bead. Even if the SA collapsed, a part of the fragments survived in the microcapsules because the membrane layer wrapped around the core. This is the reason why the weight of SA-C increased significantly after 2 days. The structure gradually become fragile and collapsed rapidly on day 20, with the chitosan layer breaking down. However, SIPN membranes have high mechanical strength and do not break easily. Therefore, the weight loss of SA-C-SIPN microcapsules was not significant. In conclusion, the SIPN hydrogel could improve the working life of microcapsules due to its physical stability. And it would be more beneficial for the practical application of QQ technology-based MBR.

3.5. Tough hydrogel shell and interlayer ensure the activity of the bacteria

Compression test was applied to characterize the mechanical robustness of microcapsules with varying shell layers. It was shown (Fig. 7a and Table S2) that when the SA and SA-C were subjected to up to 80 % compressive strains, the stress of capsules was 0.6–0.7 Mpa, with the compressing modulus (Ec) 0.11 and 0.13. However, the compressive strains of SA-SIPN and SA-C-SIPN reached 2.6 Mpa and 2.08 Mpa respectively, which corresponded to the pressure at a depth of about 200 m underwater and about 110 m under dry soil [41]. And the calculated Ec values were 0.15 and 0.19. These results indicated that the SIPN hydrogel shell could strengthen the sustained stresses dramatically. Thus, the multilayer coating of an elastically tough hydrogel surrounding the alginate core contributed to the mechanical robustness of the entire QQ microcapsule, while this phenomenon was also observed in other rigid polymer coatings [42].

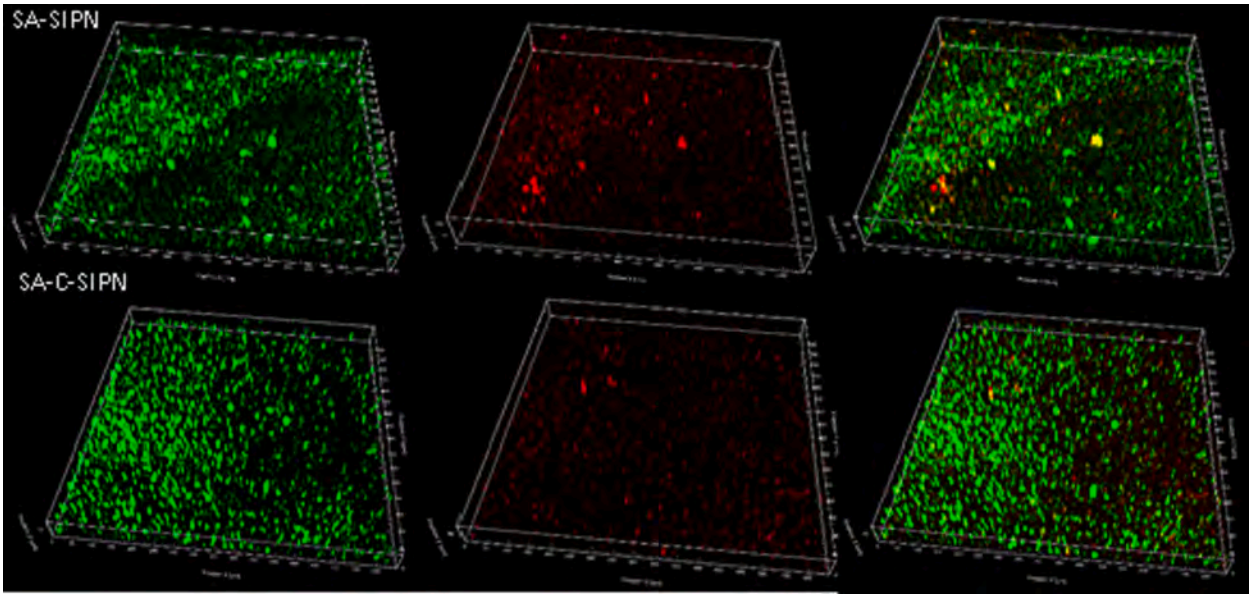

Fig. 5. CLSM image of SA-SIPN and SA-C-SIPN microcapsule.

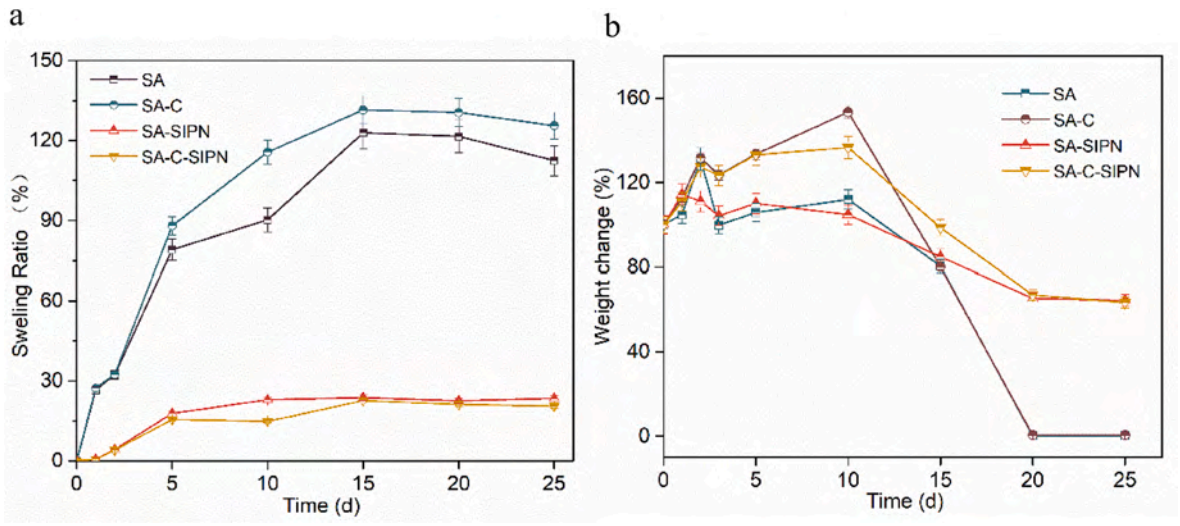

Fig. 6. (a) Swelling ratio and (b) weight change of different membrane layer beads.

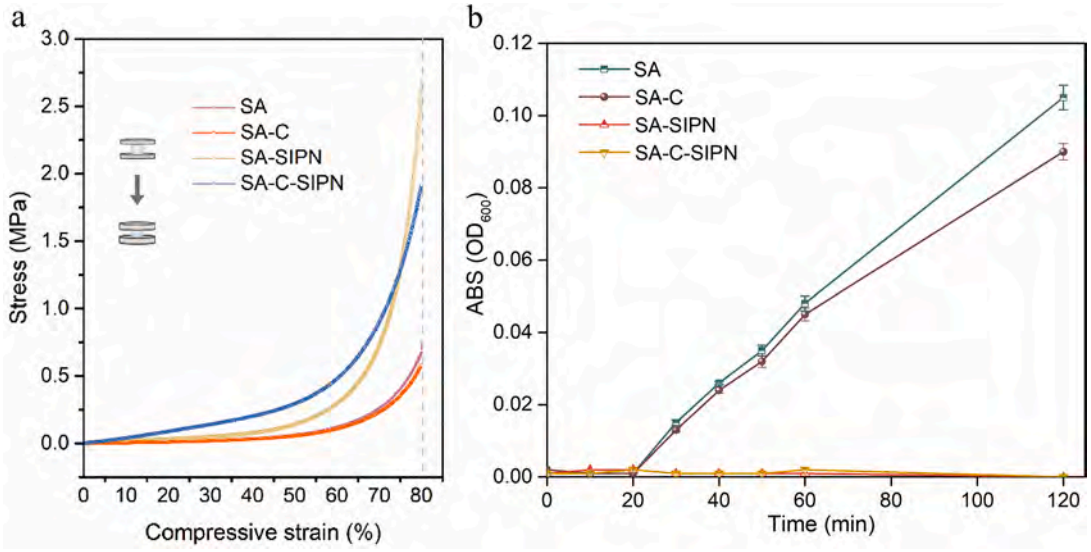

Fig. 7. (a) Effective stress–strain curves of cyclic compression of microcapsules. (b) Comparison of chemical stability of prepared microcapsules.

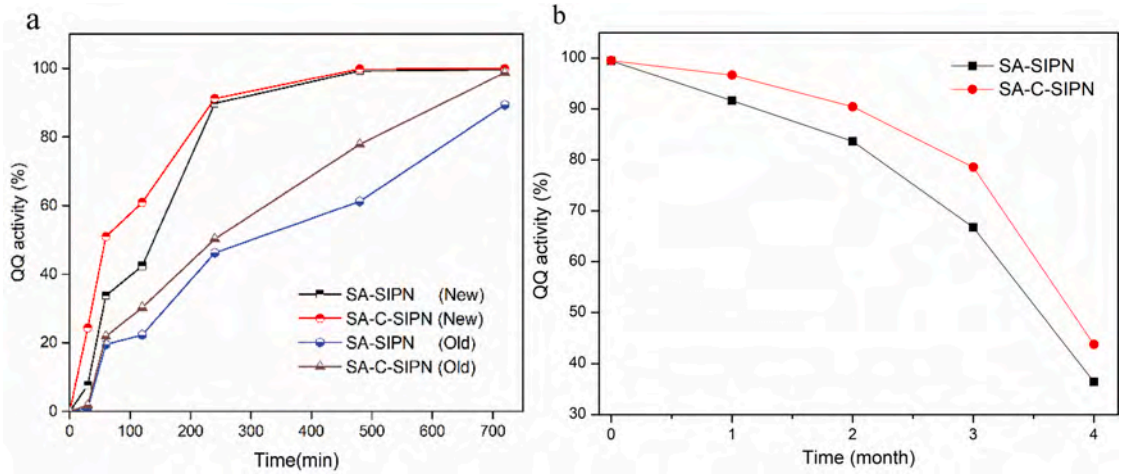

Fig. 8. (a) Short-term and (b) long-term quorum quenching activity of microcapsules (SA-SIPN and SA-C-SIPN).

Since an extreme external environment has the possibility of compromising the hydrogels and permitting bacterial escape, it was hypothesized that excellent physical containment could be imposed on the encapsulated bacteria. QQ-microcapsules were placed in EDTA buffer which simulates extreme chemical conditions, and then cell leakage was measured at OD_{600} to assess chemical stability. The results of vacant microcapsules in Fig. 7b demonstrated that only bacteria contributed to the absorption value with OD_{600}. It was presented that OD_{600} of SA and SA-C experimental groups increased rapidly from 20 min, and until the 180th minute, the BH4 bacterium immobilized in the sodium alginate core released due to the collapse of alginate cores. However, the amount of cell leakage in microcapsules coating with a SIPN membrane layer (SA-SIPN and SA-C-SIPN) is nearly negligible, so the tough shell has high chemical shock resistance for harsh chemical protection and can maintain a porous structure for a long time.

3.6. Quorum quenching efficiency of microcapsules

To evaluate the QQ activity of BH4 immobilized microcapsules, AHL-based QQ activity test and biofilm formation experiments were conducted. It was presented in Fig. 8a that the initial quorum quenching activity of the SA-C-SIPN was higher than SA-SIPN microcapsule, the C8-HSL degradation rate was 42.40 % and 60.91 % in 2 h, respectively, then reached above 99 % after 8 h. In view of the protection of the intermediate layer, the immediate positive effect in QQ activity was appeared (Petka et al., 2020), and then achieved excellent quorum quenching effect in eight hours (above 99 %). To evaluate the stability and preservation ways of the microcapsules, we monitored the quenching efficiency of the microcapsules after conventional storage at 4℃ for 3 months as old-microcapsules. The QQ activities of SA-SIPN and SA-C-SIPN old-microcapsules were 61.21 % and 77.83 % at 8 h and could still reach 99 % at the 12th hour. Therefore, the QQ activity of SA-C-SIPN was higher than that of SA-SIPN in short time, although they reached 99 % in a certain period, SA-C-SIPN could maintain a stable and efficient quenching effect.

In the long-term quorum quenching experiments (Fig. 8b), the degradation rates of C8-HSL (SA-SIPN and SA-C-SIPN) were up to 92 % and 98 % at the first month. Moreover, the quorum quenching efficiency were maintained at 66 % and 79 % respectively for nearly 100 days in the continuous aeration environment. Among them, SA-C-SIPN has more stable quorum quenching performance in the long-term operation of MBR, which indicated that the addition of chitosan layer could protect the internal bacteria availably.

To further investigate the effect of QQ capsules on biofilm, we performed simulated biofilm formation experiments to evaluate the mitigation effect of four types of microcapsules (vacant and QQ microcapsules) on membrane biofilm including physical flushing and quorum quenching effects. In Fig. S4, it was shownthat the biofilm formations in other 8 reactors were reduced in varying degrees compared with control (1.12), which illustrated that microcapsules could inhibit the biofilm to a certain extent. For vacant microcapsules, the OD590 values of four kinds of microcapsules were 0.73 (SA), 0.72 (SA-C), 0.91 (SA-SIPN), and 0.96 (SA-C-SIPN) respectively, which indicated the SA-C-SIPN microcapsules exhibited a stronger physical flushing effect in the biofilm formation process. In general, fouling mitigation has been reported to be positively correlated with the diameter of the QQ medium in physical washing research [43], hence the two types of microcapsules with larger radius (SA-SIPN and SA-C-SIPN) showed a more pronounced physical scouring on the biofilm. However, SA-C-SIPN-QQ microcapsule presented superior anti-biofouling performance, the biofilm formation was about 9.7 % and 47.3 % lower than vacant SA-C-SIPN microcapsule and control respectively, thus the anti-biofouling effect of SA-C-SIPN-QQ microcapsule was mainly the combined effect of physical scouring and quorum quenching activity.

3.7. Effects of hydrogel microcapsules on MBR performance

3.7.1. MBR performance

Quality assurance of the effluent after product dosing is a key aspect. The effects of microcapsules on the performance of MBR were presented in Fig. 9, the COD and TN removal efficiency maintained at relatively high levels throughout the period in three reactors (Almost all above 90 %) which illustrated QQ-microcapsule did not make any significant different on the treatment efficiency of COD and TN. However, the effluent concentration of PO_4^{3-} in vacant-microcapsule MBR and QQ-microcapsule MBR were lower than the control MBR during the two phases, in details, 20.53 % and 45.16 % lower in 12th day, 9.19 % and 9.20 % lower in 27th day, the prepared SA-C-SIPN microcapsule, especially QQ microcapsule, showed the potential to promote phosphorus removal. According to previous study, co-precipitation mode with co-agulants such as PAM is often used in MBR processes to improve phosphorus removal [44], moreover, chemically enhanced primary treatment (CEPT) is an effective approach which use chemical co-agulants to enhance the coagulation or flocculation of wastewater particles. To demonstrate the enhanced removal of phosphorus by PAM, we conducted a static adsorption experiment in Fig. S4, the adsorption of PO_4^{3-} with 2 % SA-C-SIPN liquor occurs quickly initially within 0.5 h in the Milli-Q water, and the adsorption equilibrium was sufficiently reached in 24 h. Therefore, not only does the SIPN shell protect inner quorum quenching bacteria, PAM components in the structure could transform PO_4^{3-} in wastewater into solid due to the flocculation and adsorption with enhancing the effect of phosphorus removal.

3.7.2. Membrane filtration performance and biofilm formation

The membrane filtration performance of microcapsules with and without QQ addition was evaluated to control biofouling, and the corresponding transmembrane pressure accumulation (biofouling) curves are shown in Fig. 10. At the first phase, the almost identical TMP profiles of three reactors illustrated that the microbial growth and operating parameters of the three reactors were generally the same. Afterwards, an equal number of vacant microcapsules and QQ microcapsules were injected into the reactors and the control reactor was run in parallel. During the dosing cycle of microcapsules, the Control MBR underwent a rapid TMP growth and reached 40 kPa within 5 ~ 6 days. Meanwhile, it took 13 ~ 14 days to reach TMP of 40 kPa for the Vacant microcapsule MBR in which only the physical cleaning effect would be expected through scouring between moving vacant microcapsules and hollow fiber membrane surfaces. And the QQ microcapsule MBR had the slowest TMP growth (19 ~ 20 days) due to the combination of quorum quenching and physical scouring. It was summarized that the QQ microcapsule deferred the biofouling rate 233 %-280 % compared to the control MBR.

The quorum quenching effect of microcapsules in MBR was confirmed by analyzing of EPS content and visualizing membrane biofilm using CLSM. Table S3 exposed the SMP and EPS content of the sludge mixture in the three MBRs. Among them, the concentrations of SMP in vacant-microcapsule MBR and QQ-microcapsule MBR were 8.06 mg/ L and 5.57 mg/ L, which was reduced by 12.9 % and 39.7 % compared with the concentration in Control MBR, respectively. Accordingly, LB-EPS and TB-EPS in QQ-microcapsule MBR decreased 57.47 % and 34.89 % compared with Control MBR. Therefore, the application of QQ-microcapsule inhibited quorum sensing between cells by reducing the AHL, thereby decreasing SMP and EPS production in MBRs.

Fig. 11 showed the CLSM reconstruction image of the biofilm formed on the surface of the MBR membrane component after the end of the running cycle. The amount of biofilm formation in the MBR with QQ microcapsule was the least (Fig. 11c), and was the most the amount of biofilm formation in the control MBR (Fig. 11a), and the amount of biofilm formation in the vacant microcapsule MBR was medium (Fig. 11b). In summary, QQ microcapsule cause physiological changes in

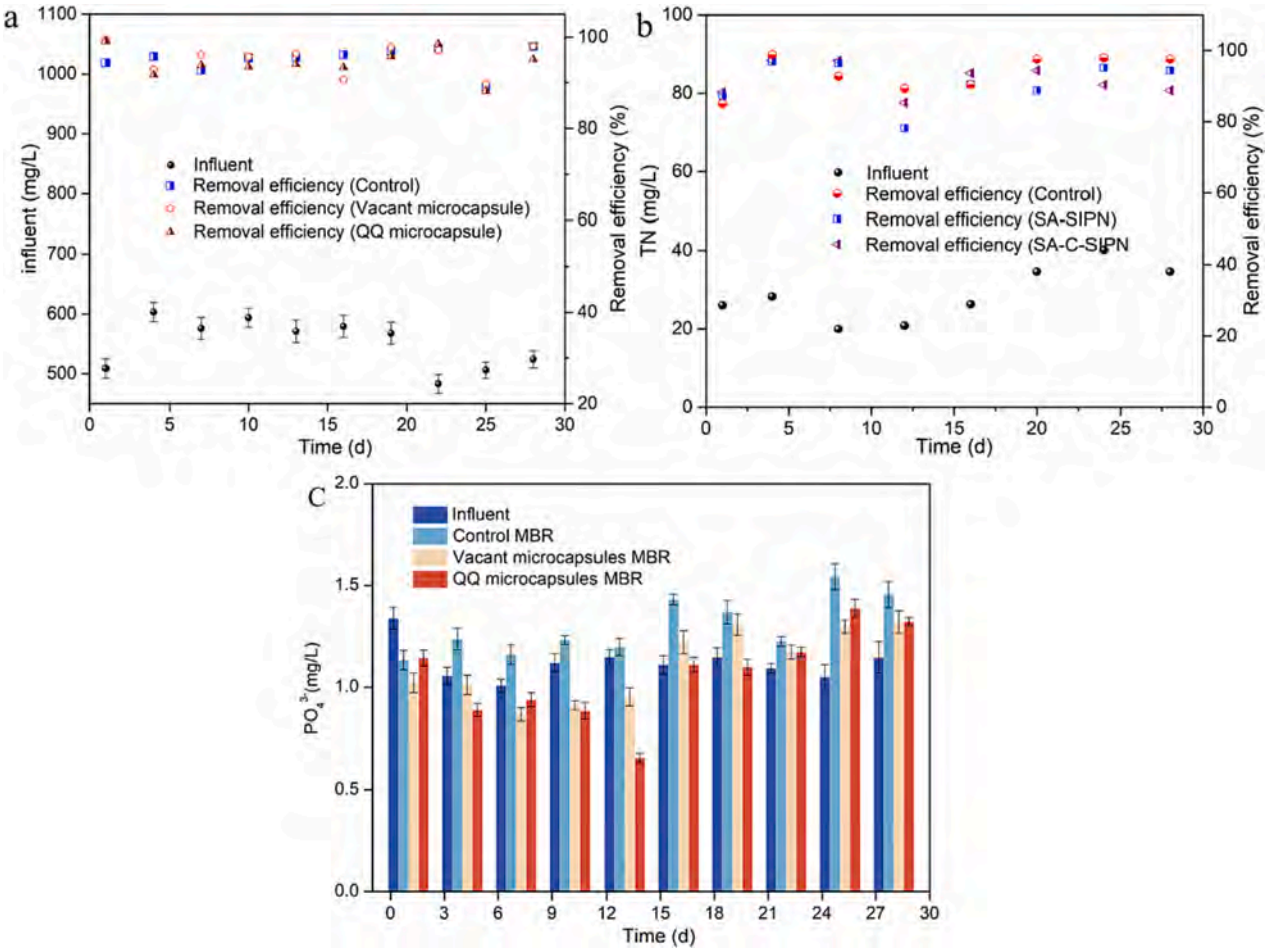

Fig. 9. Effect of vacant-microcapsules and QQ-microcapsules on MBR performance of: (a) COD removal. (b) TN removal. (c) PO_4^{3-} removal.

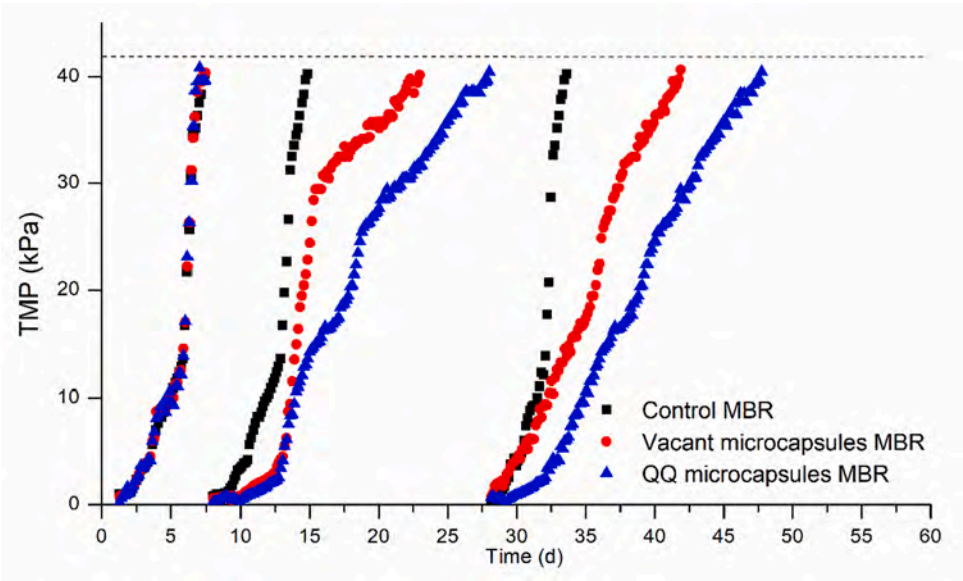

Fig. 10. TMP profiles during the operation of continuous MBR in three cycles.

microorganisms, including reduced EPS production by blocking AHL formation and disruption, resulting in reduced intercellular cohesion or cell-membrane adhesion, and therefore, less biomass adhering to the membrane.

4. Conclusion

A microcapsule product with coupling quenching sterilization and pollutant removal enhancement was successfully prepared, and its anti-

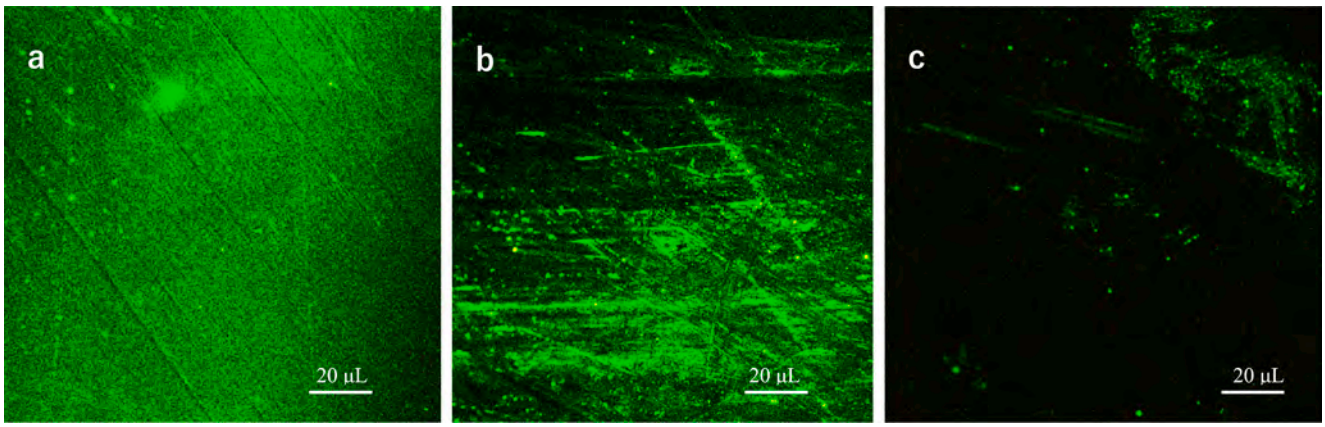

Fig. 11. The CLSM images of the biofouling on the membrane surfaces in (a) the Control MBR, (b) Vacant microcapsules MBR and (c) QQ microcapsules MBR after the TMP of QQ microcapsules MBR reached 40 kPa.

membrane biofouling and obvious phosphorus adsorption effect were verified in the continuous MBRs. The following conclusions were made.

(1) A stable core–shell encapsulated bacterium structure was fabricated by crosslinking/ embedding/film coating method, which could make the production standardization.
(2) Herein, the QQ-microcapsule enables near-perfect biocontainment and shows stable physical and chemical stability performance under harsh environmental. Thus, it was successfully used for biofouling control by interspecies interference in MBR.
(3) The treatment efficiency especially phosphorus removal efficiency was enhanced in MBR was observed because the shell material was a kind of commonly used flocculant in wastewater treatment.
(4) The simplified production process, enhanced stability and performance improvement in lab setup of QQ media, can contribute significantly to the application of QQ bacteria for the anti-biofouling process in actual MBR system.

CRediT authorship contribution statement

Kaixin Yi: Writing – review & editing, Writing – original draft, Investigation, Data curation. **Jinhui Huang:** Project administration, Conceptualization. **Haoliang Pang:** Writing – review & editing, Software. **Suzhou Li:** Investigation, Formal analysis. **Zhexi Liu:** Supervision, Investigation. **Xia Wang:** Writing – review & editing, Conceptualization. **Wei Zhang:** Formal analysis, Conceptualization. **Chenyu Zhang:** Methodology, Data curation. **Si Liu:** Investigation, Formal analysis. **Yanling Gu:** Funding acquisition, Formal analysis.

Declaration of competing interest

The authors declare that they have no known competing financial interests or personal relationships that could have appeared to influence the work reported in this paper.

Data availability

Data will be made available on request.

Acknowledgments

This study was supported by the Water Conservancy Science and Technology Project of Hunan Province (XSKJ2022068-20), the National Natural Science Foundation of China (52000012) and the Natural Science Foundation of Hunan Province (2021JJ40578). We especially thank Professor Chung-Hak Lee of the school of Chemical and Biological Engineering, Seoul National University, Republic of Korea for supplying *Rhodococcus* sp. BH4.

Appendix A. Supplementary data

Supplementary data to this article can be found online at https://doi.org/10.1016/j.cej.2024.150103.

References

[1] L. Shi, J. Huang, L. Zhu, Y. Shi, K. Yi, X. Li, Role of concentration polarization in cross flow micellar enhanced ultrafiltration of cadmium with low surfactant concentration, Chemosphere 237 (2019) 124859.
[2] Y. Shi, J. Huang, G. Zeng, Y. Gu, Y. Chen, Y. Hu, B. Tang, J. Zhou, Y. Yang, L. Shi, Exploiting extracellular polymeric substances (EPS) controlling strategies for performance enhancement of biological wastewater treatments: an overview, Chemosphere 180 (2017) 396–411.
[3] J. Huang, K. Yi, G. Zeng, Y. Shi, Y. Gu, L. Shi, H. Yu, The role of quorum sensing in granular sludge: impact and future application: a review, Chemosphere 236 (2019), https://doi.org/10.1016/j.chemosphere.2019.07.041.
[4] S. Uroz, S.R. Chhabra, M. Camara, P. Williams, P. Oger, Y. Dessaux, N-acylhomoserine lactone quorum-sensing molecules are modified and degraded by *Rhodococcus erythropolis* W2 by both amidolytic and novel oxidoreductase activities, Microbiol.-SGM 151 (2005) 3313–3322, https://doi.org/10.1099/mic.0.27961-0.
[5] H.-S. Oh, K.-M. Yeon, C.-S. Yang, S.-R. Kim, C.-H. Lee, S.Y. Park, J.Y. Han, J.-K. Lee, Control of membrane biofouling in mbr for wastewater treatment by quorum quenching bacteria encapsulated in microporous membrane, Environ. Sci. Tech. 46 (9) (2012) 4877–4884, https://doi.org/10.1021/es204312u.
[6] Y. Ouyang, Y. Hu, J. Huang, Y. Gu, Y. Shi, K. Yi, Y. Yang, Effects of exogenous quorum quenching on microbial community dynamics and biofouling propensity of activated sludge in MBRs, Biochem. Eng. J. 157 (2020), https://doi.org/10.1016/j.bej.2020.107534.
[7] T.B. Rasmussen, M. Givskov, Quorum sensing inhibitors: a bargain of effects, Microbiol.-SGM 152 (2006) 895–904, https://doi.org/10.1099/mic.0.28601-0.
[8] J. Huang, Y. Yang, G. Zeng, Y. Gu, Y. Shi, K. Yi, Y. Ouyang, J. Hu, L. Shi, Membrane layers intensifying quorum quenching alginate cores and its potential for membrane biofouling control, Bioresour. Technol. 279 (2019) 195–201.
[9] C.H. Nahm, D.-C. Choi, H. Kwon, S. Lee, S.H. Lee, K. Lee, K.-H. Choo, J.-K. Lee, C.-H. Lee, P.-K. Park, Application of quorum quenching bacteria entrapping sheets to enhance biofouling control in a membrane bioreactor with a hollow fiber module, J. Membr. Sci. 526 (2017) 264–271, https://doi.org/10.1016/j.memsci.2016.12.046.
[10] T. Lan, J. Huang, Y. Ouyang, K. Yi, H. Yu, W. Zhang, C. Zhang, S. Li, QQ-PAC core-shell structured quorum quenching beads for potential membrane antifouling properties, Enzyme Microb. Tech. 148 (2021), https://doi.org/10.1016/j.enzmictec.2021.109813.
[11] J.S. Singh, P.C. Abhilash, H.B. Singh, R.P. Singh, D.P. Singh, Genetically engineered bacteria: an emerging tool for environmental remediation and future research perspectives, Gene 480 (1–2) (2011) 1–9, https://doi.org/10.1016/j.gene.2011.03.001.
[12] A.S. Hoffman, Hydrogels for biomedical applications, Adv. Drug Deliver Rev. 54 (1) (2002) 3–12, https://doi.org/10.1016/s0169-409x(01)00239-3.
[13] M. Choi, J. Choi, S. Kim, S. Nizamoglu, S.K. Hahn, S.H. Yun, Light-guiding hydrogels for cell-based sensing and optogenetic synthesis in vivo, Nat. Photonics 7 (12) (2013) 987–994, https://doi.org/10.1038/nphoton.2013.278.

[14] A.C. Anselmo, K.J. McHugh, J. Webster, R. Langer, A. Jaklenec, Layer-by-layer encapsulation of probiotics for delivery to the microbiome, Adv. Mater. 28 (43) (2016) 9486-+, https://doi.org/10.1002/adma.201603270.
[15] K.Y. Lee, D.J. Mooney, Alginate: properties and biomedical applications, Prog. Polym. Sci. 37 (1) (2012) 106–126, https://doi.org/10.1016/j.progpolymsci.2011.06.003.
[16] C.J. Kearney, D.J. Mooney, Macroscale delivery systems for molecular and cellular payloads, Nat. Mater. 12 (11) (2013) 1004–1017, https://doi.org/10.1038/nmat3758.
[17] S.-R. Kim, K.-B. Lee, J.-E. Kim, Y.-J. Won, K.-M. Yeon, C.-H. Lee, D.-J. Lim, Macroencapsulation of quorum quenching bacteria by polymeric membrane layer and its application to MBR for biofouling control, J. Membrane Sci. 473 (2015) 109–117, https://doi.org/10.1016/j.memsci.2014.09.009.
[18] Z. Liu, Y. Jiao, Y. Wang, C. Zhou, Z. Zhang, Polysaccharides-based nanoparticles as drug delivery systems, Adv. Drug Deliver Rev. 60 (15) (2008) 1650–1662, https://doi.org/10.1016/j.addr.2008.09.001.
[19] J. Huang, L. Zhu, G. Zeng, L. Shi, Y. Shi, K. Yi, X. Li, Recovery of Cd(II) and surfactant in permeate from MEUF by foam fractionation with anionic-nonionic surfactant mixtures, Colloid Surf. A 570 (2019) 81–88, https://doi.org/10.1016/j.colsurfa.2019.03.010.
[20] X. Liu, T.-C. Tang, E. Tham, H. Yuk, S. Lin, T.K. Lu, X. Zhao, Stretchable living materials and devices with hydrogel–elastomer hybrids hosting programmed cells, P. Natl. A Sci. 114 (9) (2017) 2200–2205, https://doi.org/10.1073/pnas.1618307114.
[21] Y. Liu, M.H. Rafailovich, R. Malal, D. Cohn, D. Chidambaram, Engineering of bio-hybrid materials by electrospinning polymer-microbe fibers, Engineering of bio-hybrid materials by electrospinning polymer-microbe fiber. 106(34) (2009) 14201-14206.
[22] W.A. Shewa, M. Dagnew, Revisiting chemically enhanced primary treatment of wastewater: A review. Sustainability. 12(15). 5928.
[23] W. Yu, H. Song, G. Zheng, X. Liu, Y. Zhang, X. Ma, Study on membrane characteristics of alginate-chitosan microcapsule with cell growth, J Membrane Sci. 377 (1–2) (2011) 214–220, https://doi.org/10.1016/j.memsci.2011.04.053.
[24] D.C. Harris, Quantitative chemical analysis, Macmillan, 2010.
[25] J. Huang, Y. Gu, G. Zeng, Y. Yang, Y. Ouyang, L. Shi, Y. Shi, K. Yi, Control of indigenous quorum quenching bacteria on membrane biofouling in a short-period MBR, Bioresour. Technol. 283 (2019) 261–269, https://doi.org/10.1016/j.biortech.2019.03.082.
[26] Z. Liu, H. Pang, K. Yi, X. Wang, W. Zhang, C. Zhang, S. Liu, Y. Gu, J. Huang, L. Shi, Isolation and application of Bacillus thuringiensis LZX01: efficient membrane biofouling mitigation function and anti-toxicity potential, Bioresour. Technol. 130272 (2024).
[27] S.H. Lee, S. Lee, K. Lee, C.H. Nahm, H. Kwon, H.-S. Oh, Y.-J. Won, K.-H. Choo, C.-H. Lee, P.-K. Park, More efficient media design for enhanced biofouling control in a membrane bioreactor: quorum quenching bacteria entrapping hollow cylinder, Environ. Sci. Tech. 50 (16) (2016) 8596–8604, https://doi.org/10.1021/acs.est.6b01221.
[28] K. Yi, Y. Ouyang, J. Huang, H. Pang, C. Liu, W. Shu, C. Ye, J. Guo, Evaluating the effect of aeration rate on quorum quenching membrane bioreactors: performance of activated sludge, membrane fouling behavior, and the energy consumption analysis, J. Environ. Chem. Engin. 11 (1) (2023) 109037, https://doi.org/10.1016/j.jece.2022.109037.
[29] L. Shi, J. Huang, G. Zeng, L. Zhu, Y. Gu, Y. Shi, K. Yi, X. Li, Roles of surfactants in pressure-driven membrane separation processes: a review, Environ. Sci. Pollut. Res. 26 (30) (2019) 30731–30754, https://doi.org/10.1007/s11356-019-06345-x.
[30] S. Liu, J. Huang, W. Zhang, L. Shi, K. Yi, C. Zhang, H. Pang, J. Li, S. Li, Investigation of the adsorption behavior of Pb (II) onto natural-aged microplastics as affected by salt ions, J. Hazard. Mater. 431 (2022) 128643.
[31] G. Orive, S.K. Tam, J.L. Pedraz, J.-P. Hallé, Biocompatibility of alginate–poly-l-lysine microcapsules for cell therapy, Biomaterials 27 (20) (2006) 3691–3700.
[32] L.H. Keith, Compilation of EPA's sampling and analysis methods, CRC Press, 1996.
[33] H. Yu, J. Huang, L. Jiang, X. Yuan, K. Yi, W. Zhang, J. Zhang, H. Chen, Steering photo-excitons towards active sites: intensified substrates affinity and spatial charge separation for photocatalytic molecular oxygen activation and pollutant removal, Chem. Eng. J. 408 (2021) 127334.
[34] https://doi.org/Zhang, Miqin/0000-0001-8974-1494.
[35] Z.S. Li, H.R. Ramay, K.D. Hauch, D.M. Xiao, M.Q. Zhang, Chitosan-alginate hybrid scaffolds for bone tissue engineering, Biomaterials 26 (18) (2005) 3919–3928, https://doi.org/10.1016/j.biomaterials.2004.09.062.
[36] S. Mandal, S.K. Basu, B. Sa, Ca2+ ion cross-linked interpenetrating network matrix tablets of polyacrylamide-grafted-sodium alginate and sodium alginate for sustained release of diltiazem hydrochloride, Carbohyd. Polym. 82 (3) (2010) 867–873, https://doi.org/10.1016/j.carbpol.2010.06.009.
[37] A. Sand, M. Yadav, D.K. Mishra, K. Behari, Modification of alginate by grafting of N-vinyl-2-pyrrolidone and studies of physicochemical properties in terms of swelling capacity, metal-ion uptake and flocculation, Carbohyd. Polym. 80 (4) (2010) 1147–1154, https://doi.org/10.1016/j.carbpol.2010.01.036.
[38] D. Solpan, M. Torun, G. Gueven, The usability of (sodium alginate/acrylamide) semi-interpenetrating polymer networks on removal of some textile dyes, J. Appl. Polym. Sci. 108 (6) (2008) 3787–3795, https://doi.org/10.1002/app.27945.
[39] N. Boskovic-Vragolovic, R. Garic-Grulovic, Z. Grbavcic, R. Pjanovic, Mass transfer and fluid flow visualization in packed and fluidized beds by the adsorption method, Russ. J. Phys. Chem. A 83 (9) (2009) 1550–1553, https://doi.org/10.1134/s0036024409090246.
[40] H.S. Samanta, S.K. Ray, Synthesis, characterization, swelling and drug release behavior of semi-interpenetrating network hydrogels of sodium alginate and polyacrylamide, Carbohyd. Polym. 99 (2014) 666–678.
[41] J. Atkinson, The mechanics of soils and foundations, CRC press 2017.
[42] B.C. Zarket, S.R. Raghavan, Onion-like multilayered polymer capsules synthesized by a bioinspired inside-out technique, Nat. Commun. 8 (2017), https://doi.org/10.1038/s41467-017-00077-7.
[43] M. Aslam, P.L. McCarty, J. Bae, J. Kim, The effect of fluidized media characteristics on membrane fouling and energy consumption in anaerobic fluidized membrane bioreactors, Sep. Purif. Technol. 132 (2014) 10–15.
[44] S.-Q. Xia, D.-H. Yang, B. Xu, J.-F. Zhao, Chemical and biological flocculation process to treat municipal sewage and analysis of biological function, J. Environ. Sci. 17 (1) (2005) 163–167.